

# On the running coupling in the JIMWLK equation

T. Lappi<sup>1,2</sup> and H. Mäntysaari<sup>1</sup>

<sup>1</sup> *Department of Physics, P.O. Box 35, 40014 University of Jyväskylä, Finland*

<sup>2</sup> *Helsinki Institute of Physics, P.O. Box 64, 00014 University of Helsinki, Finland*

We propose a new method to implement the running coupling constant in the JIMWLK equation, imposing the scale dependence on the correlation function of the random noise in the Langevin formulation. We interpret this scale choice as the transverse momentum of the emitted gluon in one step of the evolution and show that it is related to the “Balitsky” prescription for the BK equation. This slows down the evolution speed of a practical solution of the JIMWLK equation, bringing it closer to the  $x$ -dependence inferred from fits to HERA data. We further study our proposal by a numerical comparison of the BK and JIMWLK equations.

PACS numbers: 24.85.+p, 12.38.Lg

## I. INTRODUCTION

To understand hadronic and nuclear scattering at the high collision energies reached at the LHC, one needs a good picture of high energy behavior of QCD. Much of the phenomenological work in the field is done within the Color Glass Condensate (CGC) framework (for reviews see e.g. [1, 2]). In this picture, the most convenient choice for the basic degrees of freedom of a hadronic state are Wilson lines (path ordered exponentials of the color field), which describe the eikonal propagation of a high energy probe. In the CGC, these are stochastic variables drawn from an energy-dependent probability distribution. This energy dependence is described by the JIMWLK renormalization group equation (see Ref. [3–5]), which can be derived in weak coupling QCD by successively integrating additional gluonic degrees of freedom into the Wilson lines.

With a solution of the JIMWLK equation one can calculate expectation values for various operators formed from the Wilson lines, describing different scattering processes. For example the simplest one, the dipole, (see Eq. (10)) is related to the inclusive DIS cross section and to the unintegrated gluon distribution, needed for single inclusive particle multiplicities. In phenomenological work, the dipole can most conveniently be obtained from the Balitsky-Kovchegov (BK) equation [6–8] which, although the original derivation predates JIMWLK, can now be viewed as its mean field approximation. Multi-particle correlation observables, however, require an understanding of the JIMWLK evolution beyond the BK approximation. For example, for a calculation of the azimuthal angle dependence of two-particle correlations [9–13] one needs the expectation values of four and six point functions such as the quadrupole, Eq. (28). Another example are long range rapidity correlations, e.g. the “ridge”, which is related to long range correlations in the color fields of the colliding hadrons [14–18].

The inclusion of the running coupling constant in the BK equation (rcBK) [19–21] has been an essential theoretical improvement for phenomenological applications [22–26]. The running of the QCD coupling slows

down the evolution (with  $x$  or equivalently  $\ln \sqrt{s}$ ) significantly from the fixed coupling case, bringing the speed to a rough agreement with HERA measurements. Since the full NLO version of the equation [27] has not been extensively applied to phenomenology (see however recent work in Ref. [28]), rcBK is currently the state of the art in phenomenological applications.

The running coupling resums a certain subset of all the NLO corrections to the evolution equations. Which subset precisely one chooses to resum is not uniquely defined, but different choices lead to different “prescriptions”. Once the other NLO corrections are included, the physical result should be independent of this prescription. However, in present day applications this is not done yet, and the result will depend on how the running coupling is implemented. The running coupling constant prescription that is usually used with the BK equation is the one derived by Balitsky [20] (our Eq. (38)), since it has been found to minimize a certain subset of other NLO contributions [21] and provide a slow evolution speed roughly consistent with HERA data.

The few existing solutions [11, 29] of the JIMWLK equation with a running coupling have not used the same prescription. This is due to the need to decompose the evolution kernel into a product of two factors for the numerical solution of the JIMWLK equation. Instead, what has been used is a “square root” running coupling, Eq. (15). What we propose in this paper as a solution to overcome this technical limitation is an alternative form of the running coupling JIMWLK equation, given by Eqs. (25) and (26).

In this paper our starting point is different from Refs. [19–21], where one sets out to find the correct modification of the BK kernel, keeping the form of the BK equation otherwise intact. Here we want to propose an equation (“rcJIMWLK”) that keeps intact the functional form of the JIMWLK equation and there is no particular reason for the resulting mean field BK approximation to stay exactly the same. We will, however, argue the BK equation derived from our proposal (Eq. (27)) is for practical purposes very close to the one with the Balitsky prescription. Its functional form is also, while different from rcBK, not that different from structures appear-

ing in the full NLO BK equation. We will also compare numerical simulations of both the BK equation and our proposed JIMWLK formulation, starting from the same initial condition.

This paper is organized in the following way. We shall first, in Sec. II, recall the Langevin formulation of the JIMWLK equation existing in the literature and in Sec. III the derivation of the BK equation from it. We proceed in Sec. IV to rewrite the Langevin step in a simpler way that corresponds to the manifestly left-right or “mirror” [30–32] symmetric form of JIMWLK. We then motivate our proposal for a running coupling version of the equation in Sec. V and discuss its relation to the rcBK equation in Sec. VI. In Sec. VII we compare numerical solutions of the rcBK and rcJIMWLK equations before concluding in Sec. VIII.

## II. LANGEVIN FORMULATION OF JIMWLK

The equation for the probability distribution of Wilson lines can be seen as a functional Fokker-Planck equation [4]. This in turn can be re-expressed as a functional Langevin equation for the Wilson lines themselves [33],

$$\frac{d}{dy} V_{\mathbf{x}} = V_{\mathbf{x}} (it^a) \left[ \int_{\mathbf{z}} \varepsilon_{\mathbf{x},\mathbf{z}}^{ab,i} \xi_{\mathbf{z}}(y)_i^b + \sigma_{\mathbf{x}}^a \right]. \quad (1)$$

Here we denote two dimensional vectors by  $\mathbf{x}, \dots$  and their lengths as  $x_T$ . In the interest of space the coordinate arguments are written as subscripts. The Wilson line  $V$  is a unitary matrix in the fundamental representation, generated by  $t^a$  and  $i = 1, 2$  is a transverse spatial index. The first term in Eq. (1) is proportional to a stochastic random noise and the second one is a deterministic “drift” term. The coefficient of the noise in the stochastic term is

$$\varepsilon_{\mathbf{x},\mathbf{z}}^{ab,i} = \left( \frac{\alpha_s}{\pi} \right)^{1/2} K_{\mathbf{x}-\mathbf{z}}^i \left[ 1 - U_{\mathbf{x}}^\dagger U_{\mathbf{z}} \right]^{ab}, \quad (2)$$

which can be thought of the “square root” of the JIMWLK Hamiltonian. We follow here the notation of Ref. [11] and denote the adjoint representation Wilson line by  $U$ ; it is related to the fundamental one by

$$U_{\mathbf{x}}^{ab} = 2 \text{Tr } t^a V_{\mathbf{x}} t^b V_{\mathbf{x}}^\dagger. \quad (3)$$

We have denoted the coordinate dependent part of the kernel (essentially the  $q \rightarrow qg$  splitting wavefunction in LC quantization) by  $K_{\mathbf{x}-\mathbf{z}}^i$ . For the fixed coupling continuum theory it is simply

$$K_{\mathbf{x}-\mathbf{z}}^i = \frac{(\mathbf{x}-\mathbf{z})^i}{(\mathbf{x}-\mathbf{z})^2}; \quad \mathbf{K}_{\mathbf{x}} = \frac{\mathbf{x}}{x_T^2}. \quad (4)$$

In the “square root” prescription one would modify this to account for the running coupling, and on a lattice one needs to render  $\mathbf{K}_{\mathbf{x}-\mathbf{z}}$  consistent with periodic boundary

conditions. For this reason we will for the moment keep this more general notation. The noise  $\xi = (\xi_1^a t^a, \xi_2^a t^a)$  is taken to be Gaussian and local in color, transverse coordinate and rapidity  $y$  (evolution time) with  $\langle \xi_{\mathbf{x}}(y)_i^b \rangle = 0$  and

$$\langle \xi_{\mathbf{x}}(y)_i^a \xi_{\mathbf{y}}(y')_j^b \rangle = \delta^{ab} \delta^{ij} \delta_{\mathbf{x}\mathbf{y}}^{(2)} \delta(y-y'). \quad (5)$$

The deterministic term is

$$\sigma_{\mathbf{x}}^a = -i \frac{\alpha_s}{2\pi^2} \int_{\mathbf{z}} S_{\mathbf{x}-\mathbf{z}} \widetilde{\text{Tr}} \left[ T^a U_{\mathbf{x}}^\dagger U_{\mathbf{z}} \right], \quad (6)$$

where  $T^a$  is a generator of the adjoint representation,  $\widetilde{\text{Tr}}$  the adjoint representation trace and we have introduced the kernel

$$S_{\mathbf{x}-\mathbf{z}} = \frac{1}{(\mathbf{x}-\mathbf{z})^2}. \quad (7)$$

The Langevin process is both derived [33] and implemented numerically [34, 35] in a discrete evolution time. It is therefore useful to see explicitly what happens on one step in rapidity from  $y_n$  to  $y_{n+1} = y_n + dy$ . The change in the Wilson line is

$$V_{\mathbf{x}}(y + dy) = V_{\mathbf{x}}(y) \times \exp \left\{ it^a \int_{\mathbf{z}} \varepsilon_{\mathbf{x},\mathbf{z}}^{ab,i} \xi_{\mathbf{z}}^{b,i} \sqrt{dy} + \sigma_{\mathbf{x}}^a dy \right\}. \quad (8)$$

Note that the rapidity delta function in Eq. (5) becomes a Kronecker delta divided by the magnitude of the timestep  $\delta(y_m - y_n) \rightarrow \delta_{m,n}/dy$ , which we have removed from the normalization of the noise to keep the power counting in  $dy$  more explicit. Thus the variance of the Gaussian noise is now

$$\langle \xi_{\mathbf{x}}(m)_i^a \xi_{\mathbf{y}}(n)_j^b \rangle = \delta^{ab} \delta^{ij} \delta_{\mathbf{x}\mathbf{y}}^{(2)} \delta_{mn}, \quad (9)$$

and the stochastic term in Eq. (8) is explicitly proportional to  $\sqrt{dy}$ . The step in rapidity  $dy$  is assumed to be small so that we can expand all the quantities on one timestep to the order  $dy$ , i.e. to second order in the stochastic term and to first order in the deterministic term.

## III. DERIVING BK FROM JIMWLK AT FIXED COUPLING

The BK equation describes the time evolution of the two point function or “dipole”

$$\langle \hat{D}_{\mathbf{x},\mathbf{y}} \rangle = \frac{1}{N_c} \left\langle \text{Tr } V_{\mathbf{x}}^\dagger V_{\mathbf{y}} \right\rangle. \quad (10)$$

It can be derived from JIMWLK in a mean field approximation, where four point functions of Wilson lines are assumed to factorize into products of two point functions; what matters here is, however, not this truncation of the

Balitsky hierarchy but the relation between the BK and JIMWLK kernels. Let us start by rederiving the BK equation directly from Eq. (8). In order to get the rapidity derivative of  $\hat{D}_{\mathbf{x},\mathbf{y}}$  we must express  $\hat{D}_{\mathbf{x},\mathbf{y}}(y + dy)$  as  $\hat{D}_{\mathbf{x},\mathbf{y}}(y)$  plus a correction proportional to  $dy$ . This is done by inserting the timestep (8) into the expression for  $\hat{D}_{\mathbf{x},\mathbf{y}}(y + dy)$  and expanding to order  $dy$ . Since we are, in the BK equation, interested only in the evolution of the mean scattering amplitude we can then take an expectation value over the stochastic noise  $\xi$ , which is independent of the Wilson lines from the previous steps

in rapidity (i.e. the Langevin equation is discretized with the Itô interpretation). One then uses the Fierz identity

$$t^a M t^a = \frac{1}{2} \text{Tr } M - \frac{1}{2N_c} M \quad (11)$$

to remove the generators remaining from the Gaussian average  $\langle \xi^a \xi^b \rangle t^a \dots t^b \dots = t^a \dots t^a \dots$ . To clarify the developments in what will follow, let us gather the terms in  $(\hat{D}_{\mathbf{x},\mathbf{y}}(y + dy) - \hat{D}_{\mathbf{x},\mathbf{y}}(y))/dy$  here one by one:

$$\begin{aligned} \frac{1}{N_c} \text{Tr } V_{\mathbf{x}}^\dagger V_{\mathbf{y}} (i\sigma_{\mathbf{y}}^a t^a) &= \frac{\alpha_s}{\pi^2} \int_{\mathbf{z}} S_{\mathbf{y}-\mathbf{z}} \frac{N_c}{4} \left\{ \frac{1}{N_c} \text{Tr } V_{\mathbf{x}}^\dagger V_{\mathbf{z}} \frac{1}{N_c} \text{Tr } V_{\mathbf{z}}^\dagger V_{\mathbf{y}} - \frac{1}{N_c} \text{Tr } V_{\mathbf{y}}^\dagger V_{\mathbf{z}} \frac{1}{N_c} \text{Tr } V_{\mathbf{z}}^\dagger V_{\mathbf{x}} V_{\mathbf{x}}^\dagger V_{\mathbf{y}} \right\} \\ \frac{1}{N_c} \text{Tr } (-i\sigma_{\mathbf{x}}^a t^a) V_{\mathbf{x}}^\dagger V_{\mathbf{y}} &= \frac{\alpha_s}{\pi^2} \int_{\mathbf{z}} S_{\mathbf{x}-\mathbf{z}} \frac{N_c}{4} \left\{ \frac{1}{N_c} \text{Tr } V_{\mathbf{x}}^\dagger V_{\mathbf{z}} \frac{1}{N_c} \text{Tr } V_{\mathbf{z}}^\dagger V_{\mathbf{y}} - \frac{1}{N_c} \text{Tr } V_{\mathbf{z}}^\dagger V_{\mathbf{x}} \frac{1}{N_c} \text{Tr } V_{\mathbf{x}}^\dagger V_{\mathbf{y}} V_{\mathbf{x}}^\dagger V_{\mathbf{z}} \right\} \\ -\frac{1}{2} \frac{1}{N_c} \text{Tr } V_{\mathbf{x}}^\dagger V_{\mathbf{y}} \left\langle \left( \int_{\mathbf{z}} t^a \varepsilon_{\mathbf{y},\mathbf{z}}^{ab,i} \xi_{\mathbf{z}}^{b,i} \right)^2 \right\rangle &= \frac{\alpha_s}{\pi^2} \int_{\mathbf{z}} \mathbf{K}_{\mathbf{y}-\mathbf{z}}^2 \frac{N_c}{4} \left\{ \frac{1}{N_c} \text{Tr } V_{\mathbf{x}}^\dagger V_{\mathbf{z}} \frac{1}{N_c} \text{Tr } V_{\mathbf{z}}^\dagger V_{\mathbf{y}} - \frac{2}{N_c} \text{Tr } V_{\mathbf{x}}^\dagger V_{\mathbf{y}} \right. \\ &\quad \left. + \frac{1}{N_c} \text{Tr } V_{\mathbf{y}}^\dagger V_{\mathbf{z}} \frac{1}{N_c} \text{Tr } V_{\mathbf{z}}^\dagger V_{\mathbf{x}} V_{\mathbf{x}}^\dagger V_{\mathbf{y}} \right\} \\ -\frac{1}{2} \frac{1}{N_c} \text{Tr } \left\langle \left( \int_{\mathbf{z}} t^a \varepsilon_{\mathbf{x},\mathbf{z}}^{ab,i} \xi_{\mathbf{z}}^{b,i} \right)^2 \right\rangle V_{\mathbf{x}}^\dagger V_{\mathbf{y}} &= \frac{\alpha_s}{\pi^2} \int_{\mathbf{z}} \mathbf{K}_{\mathbf{x}-\mathbf{z}}^2 \frac{N_c}{4} \left\{ \frac{1}{N_c} \text{Tr } V_{\mathbf{x}}^\dagger V_{\mathbf{u}} \frac{1}{N_c} \text{Tr } V_{\mathbf{z}}^\dagger V_{\mathbf{y}} - \frac{2}{N_c} \text{Tr } V_{\mathbf{x}}^\dagger V_{\mathbf{y}} \right. \\ &\quad \left. + \frac{1}{N_c} \text{Tr } V_{\mathbf{z}}^\dagger V_{\mathbf{x}} \frac{1}{N_c} \text{Tr } V_{\mathbf{x}}^\dagger V_{\mathbf{u}} V_{\mathbf{x}}^\dagger V_{\mathbf{y}} \right\} \\ \frac{1}{N_c} \text{Tr } V_{\mathbf{x}}^\dagger V_{\mathbf{y}} \left\langle t^a \varepsilon_{\mathbf{y},\mathbf{z}}^{ab,j} \xi_{\mathbf{z}}^{b,j} t^c \varepsilon_{\mathbf{x},\mathbf{u}}^{cd,i} \xi_{\mathbf{u}}^{d,i} \right\rangle &= \frac{\alpha_s}{\pi^2} \int_{\mathbf{z}} \mathbf{K}_{\mathbf{x}-\mathbf{z}} \cdot \mathbf{K}_{\mathbf{y}-\mathbf{z}} N_c \left\{ \frac{1}{N_c} \text{Tr } V_{\mathbf{x}}^\dagger V_{\mathbf{y}} - \frac{1}{N_c} \text{Tr } V_{\mathbf{x}}^\dagger V_{\mathbf{z}} \frac{1}{N_c} \text{Tr } V_{\mathbf{z}}^\dagger V_{\mathbf{y}} \right\}. \end{aligned} \quad (12)$$

The terms that are linear in the noise vanish in with the expectation value. Combining the equations above yields

$$\begin{aligned} \frac{\hat{D}_{\mathbf{x},\mathbf{y}}(y + dy) - \hat{D}_{\mathbf{x},\mathbf{y}}(y)}{dy} &= \frac{\alpha_s N_c}{2\pi^2} \int_{\mathbf{z}} \left\{ \left( \frac{S_{\mathbf{x}-\mathbf{z}} + \mathbf{K}_{\mathbf{x}-\mathbf{z}}^2}{2} + \frac{S_{\mathbf{z}-\mathbf{y}} + \mathbf{K}_{\mathbf{z}-\mathbf{y}}^2}{2} - 2\mathbf{K}_{\mathbf{x}-\mathbf{z}} \cdot \mathbf{K}_{\mathbf{z}-\mathbf{y}} \right) \frac{1}{N_c} \text{Tr } V_{\mathbf{x}}^\dagger V_{\mathbf{z}} \frac{1}{N_c} \text{Tr } V_{\mathbf{z}}^\dagger V_{\mathbf{y}} \right. \\ &\quad + \frac{1}{2} (\mathbf{K}_{\mathbf{x}-\mathbf{z}}^2 - S_{\mathbf{x}-\mathbf{z}}) \frac{1}{N_c} \text{Tr } V_{\mathbf{z}}^\dagger V_{\mathbf{x}} \frac{1}{N_c} \text{Tr } V_{\mathbf{x}}^\dagger V_{\mathbf{z}} V_{\mathbf{x}}^\dagger V_{\mathbf{y}} + \frac{1}{2} (\mathbf{K}_{\mathbf{z}-\mathbf{y}}^2 - S_{\mathbf{z}-\mathbf{y}}) \frac{1}{N_c} \text{Tr } V_{\mathbf{y}}^\dagger V_{\mathbf{z}} \frac{1}{N_c} \text{Tr } V_{\mathbf{z}}^\dagger V_{\mathbf{y}} V_{\mathbf{x}}^\dagger V_{\mathbf{y}} \\ &\quad \left. - (\mathbf{K}_{\mathbf{x}-\mathbf{z}}^2 + \mathbf{K}_{\mathbf{z}-\mathbf{y}}^2 - 2\mathbf{K}_{\mathbf{x}-\mathbf{z}} \cdot \mathbf{K}_{\mathbf{z}-\mathbf{y}}) \frac{1}{N_c} \text{Tr } V_{\mathbf{x}}^\dagger V_{\mathbf{y}} \right\}. \quad (13) \end{aligned}$$

A few remarks are in place based on an inspection of Eq. (13). Firstly, one cannot separately modify the kernels  $S$  and  $\mathbf{K}$  in order to discretize the theory or to introduce a running coupling. If the relation  $\mathbf{K}^2 = S$  is not fulfilled one introduces an additional six point correlation structure into the evolution equation of the dipole. Although this kind of higher point functions do appear in the NLO BK equation, they should be corrections at order  $\alpha_s^2$  and not present here at the leading order, fixed  $\alpha_s$  level. Secondly, the stochastic term (identifiable from the kernel  $\mathbf{K}$  instead of  $S$ ) alone gives the correct BK equation virtual term, i.e. the one with only the original

dipole on the r.h.s. The stochastic term alone, however, gives an incorrect kernel for the real term and the additional sextupole term, which are then corrected by the addition of the deterministic term. We shall show in the following that the additional complication of having to include a deterministic term is an artefact resulting from writing the evolution step only in terms of a multiplication of the Wilson line from the right (right covariant derivative). The JIMWLK equation is in fact naturally left-right-symmetric, which can be made explicit by expressing it in terms of both left and right derivatives [30–32].

The fixed coupling BK equation, included here for reference, can be obtained from Eq. (13) by setting  $S = \mathbf{K}^2$  to get

$$\partial_y \hat{D}_{\mathbf{x},\mathbf{y}}(y) = \frac{\alpha_s N_c}{2\pi^2} \int_{\mathbf{z}} \left( \mathbf{K}_{\mathbf{x}-\mathbf{z}}^2 + \mathbf{K}_{\mathbf{y}-\mathbf{z}}^2 - 2\mathbf{K}_{\mathbf{x}-\mathbf{z}} \cdot \mathbf{K}_{\mathbf{y}-\mathbf{z}} \right) \times \left[ \hat{D}(\mathbf{x}, \mathbf{z}) \hat{D}(\mathbf{z}, \mathbf{y}) - \hat{D}(\mathbf{x}, \mathbf{y}) \right]. \quad (14)$$

To obtain the BK equation for the dipole  $\langle \hat{D} \rangle$  one then closes this by the mean field approximation  $\langle \hat{D} \hat{D} \rangle \approx \langle \hat{D} \rangle \langle \hat{D} \rangle$ .

The “square root” running coupling prescription of Refs. [11, 29] was simply justified as the simplest possible modification of the kernel  $\mathbf{K}$  to include a dependence of the coupling on the distance scale. If the only modification possible is that of the kernel  $\mathbf{K}$ , one cannot impose a running of the coupling as a function of the “parent” dipole size  $|\mathbf{x} - \mathbf{y}|$ . In stead, one is left with the “square root” coupling

$$\partial_y \hat{D}_{\mathbf{x},\mathbf{y}}(y) = \frac{N_c}{2\pi^2} \int_{\mathbf{z}} \left( \alpha_s(|\mathbf{x}-\mathbf{z}|) \mathbf{K}_{\mathbf{x}-\mathbf{z}}^2 + \alpha_s(|\mathbf{y}-\mathbf{z}|) \mathbf{K}_{\mathbf{y}-\mathbf{z}}^2 - 2\sqrt{\alpha_s(|\mathbf{x}-\mathbf{z}|)\alpha_s(|\mathbf{y}-\mathbf{z}|)} \mathbf{K}_{\mathbf{x}-\mathbf{z}} \cdot \mathbf{K}_{\mathbf{y}-\mathbf{z}} \right) \times \left[ \hat{D}(\mathbf{x}, \mathbf{z}) \hat{D}(\mathbf{z}, \mathbf{y}) - \hat{D}(\mathbf{x}, \mathbf{y}) \right]. \quad (15)$$

The argument of the kernel  $\mathbf{K}$  is, however, not the only scale in the problem that the coupling can depend on. Introducing an  $\alpha_s$  into the correlation function of the noise is another option which, as we will argue in Sec. V, has a nice physical interpretation. But first it is useful to simplify the Langevin form of the equation slightly.

#### IV. SIMPLER FORM OF THE LANGEVIN STEP

The presence of the deterministic term in Eq. (1) is somewhat of an inconvenience for the discussions that will follow. It is also a relatively expensive part of the numerical solution of the equation. As discussed in Ref. [5], the deterministic term is related to the need to transform “left” and “right” covariant derivatives into each other. In the Langevin formulation this means that it is a consequence of wanting to write the evolution step as a multiplication of the Wilson line from one side. We shall now show how one can write the rapidity step with only a stochastic term by allowing for a multiplication of the Wilson line from both left and right.

In order to derive an equation that describes the whole Balitsky hierarchy, not just the evolution for the dipole, we must start by finding out what exactly is the change of a single Wilson line at point  $\mathbf{x}$  to sufficient order in  $dy$ . In the evolution step of a generic Wilson line operator  $V_{\mathbf{x}_1}^\dagger \otimes \dots \otimes V_{\mathbf{x}_n}^\dagger \otimes V_{\mathbf{y}_1} \otimes \dots \otimes V_{\mathbf{y}_n}$  one needs to know, in the limit  $dy \rightarrow 0$ , its change up to  $\mathcal{O}(dy)$ -terms; the higher ones vanish in the continuous rapidity limit. Now

a  $\mathcal{O}(dy)$ -term can come from either the product of two  $\mathcal{O}(\sqrt{dy})$ -terms from different Wilson lines, or from a  $\mathcal{O}(dy)$ -term from a single Wilson line. It follows that for a single Wilson line we must, in the Langevin timestep, keep the terms linear in the noise  $\xi$ , which could be contracted with the noise term coming from another Wilson line. One must also keep the  $\mathcal{O}(dy)$  terms, but for them one can take the expectation value of the noise term, because any correlation between them and the evolution of another Wilson line would be higher order in  $dy$ . Expanding Eq. (8) to order  $dy$  and taking the expectation value of the quadratic noise term one gets

$$V_{\mathbf{x}}(y + dy) = V_{\mathbf{x}}(y) \left[ 1 + i \frac{\sqrt{\alpha_s dy}}{\pi} \int_{\mathbf{z}} \mathbf{K}_{\mathbf{x}-\mathbf{z}} \cdot \left( \xi_{\mathbf{z}} - V_{\mathbf{x}}^\dagger V_{\mathbf{z}} \xi_{\mathbf{z}} V_{\mathbf{z}}^\dagger V_{\mathbf{x}} \right) - \frac{\alpha_s dy}{2\pi^2} \int_{\mathbf{z}} \mathbf{K}_{\mathbf{x}-\mathbf{z}}^2 \left( 2 - U_{\mathbf{x}}^\dagger U_{\mathbf{z}} - U_{\mathbf{z}}^\dagger U_{\mathbf{x}} \right)^{ab} t^a t^b + \frac{\alpha_s dy}{2\pi^2} \int_{\mathbf{z}} S_{\mathbf{x}-\mathbf{z}} \left( U_{\mathbf{x}}^\dagger U_{\mathbf{z}} - U_{\mathbf{z}}^\dagger U_{\mathbf{x}} \right)^{ab} t^a t^b \right]. \quad (16)$$

Here  $V_{\mathbf{x}}^\dagger V_{\mathbf{z}} \xi_{\mathbf{z}} V_{\mathbf{z}}^\dagger V_{\mathbf{x}}$  is simply the adjoint representation product  $t^a (U_{\mathbf{x}}^\dagger U_{\mathbf{z}})^{ab} \xi_{\mathbf{z}}^b$  written out in the fundamental representation. The terms coming from the noise and deterministic contributions can be identified from the kernels  $\mathbf{K}^2$  and  $S$  respectively. The effect of the deterministic term is to cancel  $U_{\mathbf{z}}^\dagger U_{\mathbf{x}}$  and double the other term  $U_{\mathbf{x}}^\dagger U_{\mathbf{z}}$ . Now setting  $S$  equal to  $\mathbf{K}^2$  and also expressing the remaining adjoint Wilson lines in terms of fundamental ones we can write this as

$$V_{\mathbf{x}}(y + dy) = V_{\mathbf{x}} + i \frac{\sqrt{\alpha_s dy}}{\pi} \int_{\mathbf{z}} \mathbf{K}_{\mathbf{x}-\mathbf{z}} \cdot (V_{\mathbf{x}} \xi_{\mathbf{z}} - V_{\mathbf{z}} \xi_{\mathbf{z}} V_{\mathbf{z}}^\dagger V_{\mathbf{x}}) - \frac{\alpha_s dy}{2\pi^2} \int_{\mathbf{z}} \mathbf{K}_{\mathbf{x}-\mathbf{z}}^2 (V_{\mathbf{z}} \text{Tr} V_{\mathbf{z}}^\dagger V_{\mathbf{x}} - N_c V_{\mathbf{x}}). \quad (17)$$

Up to this order in  $dy$  this is equivalent to the re-exponentiated form

$$V_{\mathbf{x}}(y + dy) = \exp \left\{ -i \frac{\sqrt{\alpha_s dy}}{\pi} \int_{\mathbf{z}} \mathbf{K}_{\mathbf{x}-\mathbf{z}} \cdot (V_{\mathbf{z}} \xi_{\mathbf{z}} V_{\mathbf{z}}^\dagger) \right\} \times V_{\mathbf{x}} \exp \left\{ i \frac{\sqrt{\alpha_s dy}}{\pi} \int_{\mathbf{z}} \mathbf{K}_{\mathbf{x}-\mathbf{z}} \cdot \xi_{\mathbf{z}} \right\}, \quad (18)$$

where we have again, in the order  $dy$  replaced  $\langle \xi^2 \rangle$  by  $\xi^2$ , the difference being higher order in  $dy$ .

Equation (18), to be compared to the earlier form (16), is the main result of this section. Now the Wilson line is multiplied from both the left and the right, and consequently there is no more drift term. In addition to having fewer separate terms to calculate, Eq. (18) is significantly faster to evaluate numerically, because it avoids the need to reconstruct the adjoint representation Wilson line in

Eq. (6). We stress that Eq. (18) is precisely equivalent to the Langevin step derived in [33] in the limit of continuous evolution time  $dy \rightarrow 0$ . The difference comes only in terms at order  $\mathcal{O}(\sqrt{dy}^3)$ , which are neglected both here and in the derivation of the original equation in Ref. [33].

Note that the multiplication by the Wilson line at the coordinate  $\mathbf{z}$  from the left is a choice related to the form of the original choice to use a right derivative in (1). One could easily move it to the right by defining a rotated noise

$$\tilde{\xi}_{\mathbf{z}} = \tilde{\xi}_{\mathbf{z}}^a t^a = V_{\mathbf{z}} \xi_{\mathbf{z}} V_{\mathbf{z}}^\dagger. \quad (19)$$

It is easy to see that the distribution of  $\tilde{\xi}_{\mathbf{z}}$  is the same as that of  $\xi_{\mathbf{z}}$ , namely

$$\langle \tilde{\xi}_{\mathbf{x}}^{a,i} \tilde{\xi}_{\mathbf{y}}^{b,j} \rangle = \delta^{ab} \delta^{ij} \delta_{\mathbf{x}-\mathbf{y}}^{(2)}. \quad (20)$$

In terms of  $\tilde{\xi}_{\mathbf{z}}$  the timestep (18) is

$$V_{\mathbf{x}}(y + dy) = \exp \left\{ -i \frac{\sqrt{\alpha_s} dy}{\pi} \int_{\mathbf{z}} \mathbf{K}_{\mathbf{x}-\mathbf{z}} \cdot \tilde{\xi}_{\mathbf{z}} \right\} \\ \times V_{\mathbf{x}} \exp \left\{ i \frac{\sqrt{\alpha_s} dy}{\pi} \int_{\mathbf{z}} \mathbf{K}_{\mathbf{x}-\mathbf{z}} \cdot (V_{\mathbf{z}}^\dagger \tilde{\xi}_{\mathbf{z}} V_{\mathbf{z}}) \right\}. \quad (21)$$

## V. SETTING THE SCALE OF THE COUPLING

Recall that the change in a general correlator of  $n$  Wilson lines in one infinitesimal step in rapidity is obtained by changing all the Wilson lines by Eq. (18), developing to order  $\xi^2$  (i.e. to order  $dy$ ) and taking the expectation values with the probability distribution of the noise  $\xi$ . Physically keeping only the quadratic order in  $\xi$  corresponds to the fact that JIMWLK is a LO evolution equation, derived by considering the emission of only one gluon. The interpretation of the contractions between two  $\xi$ 's is that one corresponds to the emission of the gluon in the amplitude and the other one in the complex conjugate. In the formulation that includes the deterministic term this interpretation is not as straightforward, since in Eq. (1) one is summing a noise term corresponding to a gluon emission amplitude and the deterministic term which is an emission probability, i.e. amplitude squared.

In order to have a better picture of the physics contained in one evolution step we shall now describe, adapting the “simple derivation of the JIMWLK equation” of Ref. [5], the contractions of the  $\xi$ 's in Eq. (18) in a diagrammatic notation. We want to apply the evolution step Eq. (18) to calculate the change of a generic Wilson line operator  $V_{\mathbf{x}_1}^\dagger \otimes \dots \otimes V_{\mathbf{x}_n}^\dagger \otimes V_{\mathbf{y}_1} \otimes \dots \otimes V_{\mathbf{y}_n}$  in an infinitesimal step in rapidity. We now have to distinguish between several different cases of how these contractions are done, drawn in Figs. 1 and 2:

- The square of the noise multiplying the Wilson line from the left corresponds to the emission and reabsorption of a gluon before interaction with the target. The noise term  $\xi_{\mathbf{z}}$  is color rotated into  $V_{\mathbf{z}} \xi_{\mathbf{z}} V_{\mathbf{z}}^\dagger$  in Eq. (18), but in the square the color rotation cancels. Thus we can express this contribution as the left diagram in Fig. 1.
- Similarly we can take the square of the  $\xi$  multiplying the Wilson line from the right. Now the noise is not color rotated, i.e. this corresponds to emission from and absorption by the Wilson line after the target, shown in the middle diagram of Fig. 1.
- We can also contract the  $\xi$  multiplying the Wilson line from the left with the one multiplying it from the right. Physically this is equivalent to the interference between gluon emission before and after the interaction with the target. In the diagrammatic notation this is expressed as a gluon being emitted before the target, propagating through it, and being reabsorbed, drawn on the right in Fig. 1.
- One can also have a contraction between the  $\xi$ 's from the step of one Wilson line at coordinate  $\mathbf{x}$  with another one at  $\mathbf{y}$ . If both  $\xi$ 's multiply the Wilson lines from the left (or the hermitean conjugates from the right), they correspond to the diagram where the gluon is emitted and absorbed before the target, the color rotations again cancel. This contribution is shown on the left of Fig. 2.
- If the contracted  $\xi$ 's are the ones to the right of the Wilson lines, we have an interference between gluon emission from two different Wilson lines after the target, as shown in the middle of Fig. 2.
- Finally we can have an interference between the emission of a gluon from the Wilson line at  $\mathbf{x}$  before the collision and from another one at  $\mathbf{y}$  after the collision, as shown on the right of Fig. 2. This corresponds to the contraction between one  $\xi$  on the left and another one on the right of a Wilson line.

If now  $\xi_{\mathbf{u}}$  corresponds to the emission of a gluon at coordinate  $\mathbf{u}$  and the other  $\xi_{\mathbf{v}}$  that it is to be contracted with is interpreted as the absorption of the same gluon, what is the physical meaning of the delta function  $\delta^2(\mathbf{u} - \mathbf{v})$  in the correlation function of the noise? The answer to this question that we propose in this paper lies in realizing that in fact the “absorption” of the gluon actually corresponds to the complex conjugate of the amplitude for gluon emission. Thus if the transverse momentum of the emitted gluon is  $\mathbf{k}$ , the amplitude is  $\sim e^{i\mathbf{k} \cdot \mathbf{u}}$  and the complex conjugate  $\sim e^{-i\mathbf{k} \cdot \mathbf{v}}$ . The delta function  $\delta^2(\mathbf{u} - \mathbf{v})$  is then a result of integrating over all possible transverse momenta of the emitted gluon in one



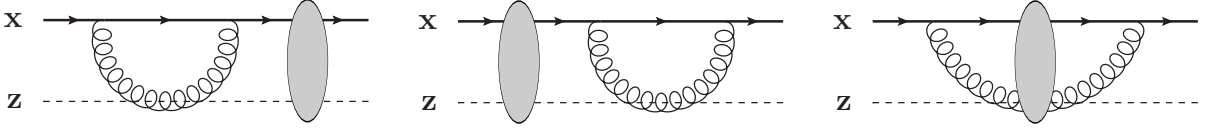


FIG. 1: Virtual diagrams.

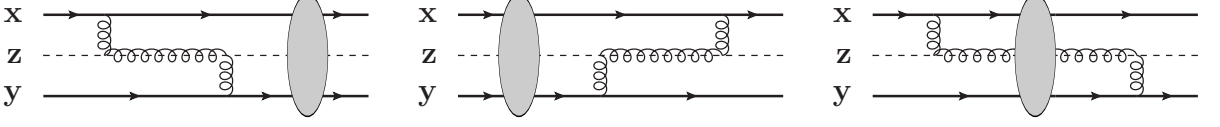


FIG. 2: Real diagrams.

step of the evolution:

$$\delta^2(\mathbf{u} - \mathbf{v}) = \int \frac{d^2\mathbf{k}}{(2\pi)^2} e^{i\mathbf{k} \cdot (\mathbf{u} - \mathbf{v})}. \quad (22)$$

The interpretation of the diagrams of Figs. 1 and 2 in terms of the transverse momentum of the gluon is shown in Figs. 3 and 4. Note that all the momenta  $\mathbf{k}$  are taken after the interaction with the target, not before. This corresponds to the choice made to use the noise  $\xi$  and not the rotated one  $\tilde{\xi}$ . The integration over the final state gluon momentum has to be done because we wish to include *all* the degrees of freedom in the rapidity interval from  $y$  to  $y + dy$  into an effective theory description of the target at the new rapidity scale  $dy$ .

What then happens if we wish to include the running coupling constant? We will here rely on the general argument in gauge theory that the beta function can be computed by considering only corrections to the gluon propagator. This is in fact the property that is used in [19, 20] to derive the running coupling constant in BK which is done by summing one loop corrections to the gluon propagator. If the running coupling corrections can be derived from just the gluon propagator, it is natural that the scale of the running coupling should be the momentum of the emitted gluon. This leads directly to our proposal for implementing the running coupling in the JIWMLK equation, which is to regard the coupling constant as a property of the correlator of the noise. We then propose to simply replace the fixed coupling correlator

$$\alpha_s \langle \xi_{\mathbf{x}}^{a,i} \xi_{\mathbf{y}}^{b,j} \rangle = \delta^{ab} \alpha_s \delta^{ij} \int \frac{d^2\mathbf{k}}{(2\pi)^2} e^{i\mathbf{k} \cdot (\mathbf{x} - \mathbf{y})} \quad (23)$$

by

$$\langle \eta_{\mathbf{x}}^{a,i} \eta_{\mathbf{y}}^{b,j} \rangle = \delta^{ab} \delta^{ij} \int \frac{d^2\mathbf{k}}{(2\pi)^2} e^{i\mathbf{k} \cdot (\mathbf{x} - \mathbf{y})} \alpha_s(\mathbf{k}), \quad (24)$$

in terms of which the rapidity step of the Wilson line is

now

$$V_{\mathbf{x}}(y + dy) = \exp \left\{ -i \frac{\sqrt{dy}}{\pi} \int_{\mathbf{u}} \mathbf{K}_{\mathbf{x}-\mathbf{u}} \cdot (V_{\mathbf{u}} \boldsymbol{\eta}_{\mathbf{u}} V_{\mathbf{u}}^\dagger) \right\} \\ \times V_{\mathbf{x}} \exp \left\{ i \frac{\sqrt{dy}}{\pi} \int_{\mathbf{v}} \mathbf{K}_{\mathbf{x}-\mathbf{v}} \cdot \boldsymbol{\eta}_{\mathbf{v}} \right\}, \quad (25)$$

with  $\boldsymbol{\eta} = (\eta_1^a t^a, \eta_2^a t^a)$ . Note that since the noise correlator is not local in transverse coordinate, we have broken the left-right symmetry of the fixed coupling equation. The physical interpretation of this is that the symmetry corresponds to time reversal, and using the momentum of a gluon in the final state after the target (as opposed to an initial state one) breaks the time reversal symmetry. While this loss of symmetry is in aesthetic, it seems inevitable at some point at least if one wants to generalize the evolution to more exclusive observables (as discussed e.g. in Ref. [36]).

Due to the FFT algorithm [37] the Fourier-transform is a relatively straightforward and inexpensive procedure on the lattice. Thus implementing the correlator (24) induces only a minor modification to the numerical algorithm [34] used to solve the JIMWLK equation. In the following we shall denote the new noise correlator by

$$\tilde{\alpha}_{\mathbf{x}-\mathbf{y}} \equiv \int \frac{d^2\mathbf{k}}{(2\pi)^2} e^{i\mathbf{k} \cdot (\mathbf{x} - \mathbf{y})} \alpha_s(\mathbf{k}). \quad (26)$$

We emphasize that the notation  $\tilde{\alpha}_{\mathbf{x}-\mathbf{y}}$  does *not* mean the coupling evaluated at the momentum scale  $1/|\mathbf{x} - \mathbf{y}|$ , but is indeed the Fourier transform of the coupling at the scale  $k_T$ . Since the coupling is a very smooth, logarithmically varying function of  $k_T$ , the transform  $\tilde{\alpha}_{\mathbf{x}-\mathbf{y}}$  is very sharply peaked around  $\mathbf{x} = \mathbf{y}$ .

## VI. RECOVERING THE BK EQUATION

Let us now calculate the change in the dipole operator during one rapidity step of the evolution. This is done by inserting Eq. (25) into the expression for  $\hat{D}_{\mathbf{x},\mathbf{y}}(y + dy)$ , developing in powers of the noise term up to  $\mathcal{O}(\eta^2)$  and

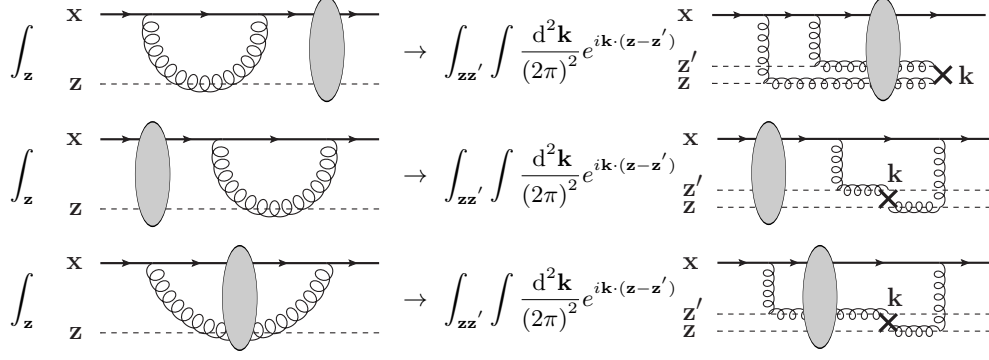


FIG. 3: Virtual diagrams in Fig. 1 rewritten with the explicit momentum argument used as the scale of the running coupling.

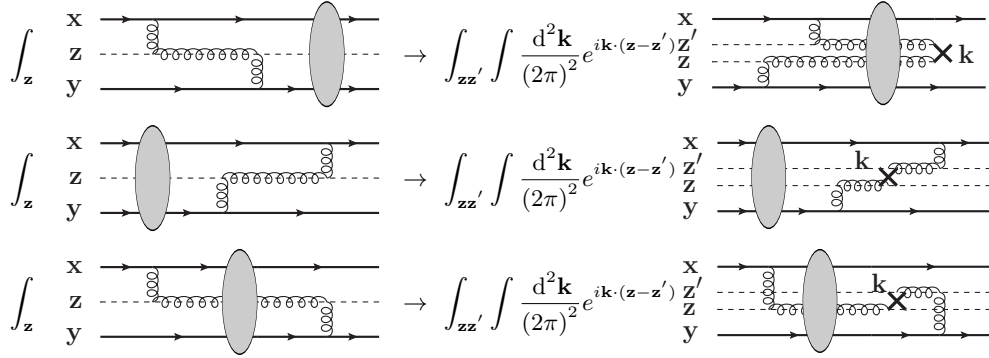


FIG. 4: Real diagrams in Fig. 2 rewritten with the explicit momentum argument used as the scale of the running coupling.

taking the expectation values with the correlator (26). The result is

---


$$\begin{aligned} \frac{\hat{D}_{\mathbf{x}-\mathbf{y}}(y+dy) - \hat{D}_{\mathbf{x}-\mathbf{y}}(y)}{dy} &= \frac{N_c}{2\pi^2} \int_{\mathbf{u}, \mathbf{v}} \tilde{\alpha}_{\mathbf{u}-\mathbf{v}} \left\{ (\mathbf{K}_{\mathbf{x}-\mathbf{u}} \cdot \mathbf{K}_{\mathbf{x}-\mathbf{v}} + \mathbf{K}_{\mathbf{y}-\mathbf{u}} \cdot \mathbf{K}_{\mathbf{y}-\mathbf{v}} - 2\mathbf{K}_{\mathbf{x}-\mathbf{u}} \cdot \mathbf{K}_{\mathbf{y}-\mathbf{v}}) \right. \\ &\quad \times \frac{1}{2} \left[ \hat{D}_{\mathbf{x}, \mathbf{u}} \hat{D}_{\mathbf{u}, \mathbf{y}} + \hat{D}_{\mathbf{x}, \mathbf{v}} \hat{D}_{\mathbf{v}, \mathbf{y}} - \hat{D}_{\mathbf{x}, \mathbf{y}} - \hat{D}_{\mathbf{v}, \mathbf{u}} \hat{Q}_{\mathbf{x}, \mathbf{v}, \mathbf{u}, \mathbf{y}} \right] \Big\}, \quad (27) \end{aligned}$$


---

where the quadrupole operator is

$$\hat{Q}_{\mathbf{x}, \mathbf{v}, \mathbf{u}, \mathbf{y}} = \frac{1}{N_c} \text{Tr} V_{\mathbf{x}}^\dagger V_{\mathbf{v}} V_{\mathbf{u}}^\dagger V_{\mathbf{y}}. \quad (28)$$

From this form it is easy to check that in the fixed coupling case  $\tilde{\alpha}_{\mathbf{u}-\mathbf{v}} = \alpha_s \delta^2(\mathbf{u}-\mathbf{v})$  we recover the usual BK equation.

Now the evolution equation for the two point function does not have the same functional form as in the fixed coupling case. Our definition of the scale of the running coupling as the momentum of the emitted final state gluon makes the position of the gluon in transverse

coordinate space different in the amplitude and the complex conjugate, resulting in a more complicated the structure for the equation. From the point of view of the full set of NLO corrections to the BK equation [27] this is not unnatural. The NLO BK equation also necessarily involves higher point dipole operators, and the definition of what subset of these corrections one chooses to call “running coupling” corrections is not unique. What is done in the derivations of the running coupling BK equation [19, 20] is that one sets out to calculate a certain subset of these NLO corrections, namely those that only modify the BK kernel, but leave the Wilson line

operator part of the BK equation intact. This particular set of NLO corrections is not necessarily one that would leave the functional form of the JIMWLK equation intact. What we are proposing here, on the other hand, is running coupling JIMWLK equation, namely an evolution equation which includes running coupling corrections, but leaves the functional form of the JIMWLK equation intact. There is no particular reason why this equation should be equivalent to a particular form of the running coupling BK equation, and indeed it is not. However, as we will show in the following, it does in fact lead to the scale of the coupling being determined by parametrically the same length scale in the parts of phase space that dominate the evolution.

In order to see the relation to rcBK equations in the literature in more detail we will now try to connect our Eq. (27), where the coupling is a function of a *momentum* scale to one where it depends on the inverse of a transverse *coordinate* distance. We shall here use the same notation for both,  $\alpha_s(\mathbf{k})$  and  $\alpha_s(\mathbf{r})$ , while deferring the explicit expressions to Sec. VII. We will also not attempt to perform the Fourier-transform from momentum to coordinate space precisely, but merely attempt to identify the dominant momentum scales in parametrically different parts of the phase space.

Let us denote  $\mathbf{z} = (\mathbf{u} + \mathbf{v})/2$  and  $\Delta\mathbf{z} = (\mathbf{u} - \mathbf{v})$ . Using the fact that  $\tilde{\alpha}_{\mathbf{u}-\mathbf{v}}$  is very peaked around  $\mathbf{u} = \mathbf{v}$  we then approximate  $\mathbf{u} \approx \mathbf{v} \approx \mathbf{z}$  (i.e. set  $\Delta\mathbf{z} = 0$ ) in the part of (27) containing the Wilson line operators

$$\frac{1}{2} \left[ \hat{D}_{\mathbf{x},\mathbf{u}} \hat{D}_{\mathbf{u},\mathbf{y}} + \hat{D}_{\mathbf{x},\mathbf{v}} \hat{D}_{\mathbf{v},\mathbf{y}} - \hat{D}_{\mathbf{x},\mathbf{y}} - \hat{D}_{\mathbf{v},\mathbf{u}} \hat{Q}_{\mathbf{x},\mathbf{v},\mathbf{u},\mathbf{y}} \right] \xrightarrow{\mathbf{u}=\mathbf{v}=\mathbf{z}} \hat{D}_{\mathbf{x},\mathbf{z}} \hat{D}_{\mathbf{z},\mathbf{y}} - \hat{D}_{\mathbf{x},\mathbf{y}}, \quad (29)$$

which is the same form as in the BK equation.

Turning then to the kernel, we can use the momentum representation of  $\mathbf{K}$

$$\mathbf{K}_{\mathbf{x}} = i(2\pi)^2 \int \frac{d^2\mathbf{k}}{(2\pi)^2} \frac{e^{-i\mathbf{k}\cdot\mathbf{x}}}{\mathbf{k}^2} \quad (30)$$

to write

$$\begin{aligned} & \int_{\Delta\mathbf{z}} \tilde{\alpha}_{\Delta\mathbf{z}} \mathbf{K}_{\mathbf{x}-\mathbf{u}} \cdot \mathbf{K}_{\mathbf{y}-\mathbf{v}} \\ &= \frac{1}{(2\pi)^2} \int_{\mathbf{p},\mathbf{q}} \alpha_s \left( \frac{\mathbf{p} + \mathbf{q}}{2} \right) \frac{\mathbf{p} \cdot \mathbf{q}}{\mathbf{p}^2 \mathbf{q}^2} e^{-i\mathbf{p}\cdot\mathbf{x} + i\mathbf{q}\cdot\mathbf{y} + i(\mathbf{p}-\mathbf{q})\cdot\mathbf{z}} \\ &= \frac{1}{(2\pi)^2} \int_{\mathbf{P},\mathbf{k}} \alpha_s(\mathbf{P}) e^{-i\mathbf{P}\cdot(\mathbf{x}-\mathbf{y}) + i\mathbf{k}\cdot(\mathbf{z} - \frac{\mathbf{x}+\mathbf{y}}{2})} \\ & \quad \times \frac{(\mathbf{P} + \mathbf{k}/2) \cdot (\mathbf{P} - \mathbf{k}/2)}{(\mathbf{P} + \mathbf{k}/2)^2 (\mathbf{P} - \mathbf{k}/2)^2} \quad (31) \end{aligned}$$

where we have changed variables from  $\mathbf{p}, \mathbf{q}$  to  $\mathbf{P} = (\mathbf{p} + \mathbf{q})/2$  and  $\mathbf{k} = \mathbf{p} - \mathbf{q}$ . Using this form we can write the

kernel of Eq. (27) as

$$\begin{aligned} & \int_{\Delta\mathbf{z}} \tilde{\alpha}_{\Delta\mathbf{z}} (\mathbf{K}_{\mathbf{x}-\mathbf{u}} \cdot \mathbf{K}_{\mathbf{x}-\mathbf{v}} + \mathbf{K}_{\mathbf{y}-\mathbf{u}} \cdot \mathbf{K}_{\mathbf{y}-\mathbf{v}} - 2\mathbf{K}_{\mathbf{x}-\mathbf{u}} \cdot \mathbf{K}_{\mathbf{y}-\mathbf{v}}) \\ &= \frac{1}{(2\pi)^2} \int_{\mathbf{P},\mathbf{k}} \alpha_s(\mathbf{P}) \frac{(\mathbf{P} + \mathbf{k}/2) \cdot (\mathbf{P} - \mathbf{k}/2)}{(\mathbf{P} + \mathbf{k}/2)^2 (\mathbf{P} - \mathbf{k}/2)^2} \\ & \quad \left[ e^{i\mathbf{k}\cdot(\mathbf{z}-\mathbf{x})} + e^{i\mathbf{k}\cdot(\mathbf{z}-\mathbf{y})} - 2e^{-i\mathbf{P}\cdot(\mathbf{x}-\mathbf{y}) + i\mathbf{k}\cdot(\mathbf{z} - \frac{\mathbf{x}+\mathbf{y}}{2})} \right]. \quad (32) \end{aligned}$$

We now look separately at two different kinematical regimes.

*a. Small daughter dipole* Let us first assume that one of the daughter dipoles is smaller, e.g.  $|\mathbf{x} - \mathbf{z}| \ll |\mathbf{y} - \mathbf{z}| \approx |\mathbf{x} - \mathbf{y}|$ . Now the dominant term in the  $\mathbf{P}$  and  $\mathbf{k}$ -integral is the one that oscillates most slowly, namely as  $e^{i\mathbf{k}\cdot(\mathbf{z}-\mathbf{x})}$ . Keeping only this term we can return to the variables  $\mathbf{p}$  and  $\mathbf{q}$  and write it as

$$\frac{1}{(2\pi)^2} \int_{\mathbf{p},\mathbf{q}} \alpha_s \left( \frac{\mathbf{p} + \mathbf{q}}{2} \right) \frac{\mathbf{p} \cdot \mathbf{q}}{\mathbf{p}^2 \mathbf{q}^2} e^{-i(\mathbf{p}-\mathbf{q})\cdot(\mathbf{x}-\mathbf{z})}. \quad (33)$$

The exponential factor now makes both  $p_T$  and  $q_T$  of the order  $1/|\mathbf{x} - \mathbf{z}|$ . We thus approximate  $\alpha_s((\mathbf{p} + \mathbf{q})/2) \approx \alpha_s(|\mathbf{x} - \mathbf{z}|)$ , leading us to the estimate

$$\sim \frac{\alpha_s(\mathbf{x} - \mathbf{z})}{(\mathbf{x} - \mathbf{z})^2}, \quad |\mathbf{x} - \mathbf{z}| \ll |\mathbf{y} - \mathbf{z}| \approx |\mathbf{x} - \mathbf{y}| \quad (34)$$

for the kernel in this limit, and similarly

$$\sim \frac{\alpha_s(\mathbf{y} - \mathbf{z})}{(\mathbf{y} - \mathbf{z})^2}, \quad |\mathbf{y} - \mathbf{z}| \ll |\mathbf{x} - \mathbf{z}| \approx |\mathbf{x} - \mathbf{y}| \quad (35)$$

for the other small daughter dipole limit. This is almost an inevitable result, which can also be seen noting that already at fixed coupling the kernel in this kinematical limit is dominated by the single term  $\mathbf{K}_{\mathbf{x}-\mathbf{z}}^2$  or  $\mathbf{K}_{\mathbf{y}-\mathbf{z}}^2$ , and the coupling must depend on the only distance scale available for it, namely the daughter dipole size.

*b. Small parent dipole* Assume then that the parent dipole is smaller, e.g.  $|\mathbf{x} - \mathbf{y}| \ll |\mathbf{x} - \mathbf{z}| \approx |\mathbf{y} - \mathbf{z}|$ . We can then approximate

$$\begin{aligned} & e^{i\mathbf{k}\cdot(\mathbf{z}-\mathbf{x})} + e^{i\mathbf{k}\cdot(\mathbf{z}-\mathbf{y})} - 2e^{-i\mathbf{P}\cdot(\mathbf{x}-\mathbf{y}) + i\mathbf{k}\cdot(\mathbf{z} - \frac{\mathbf{x}+\mathbf{y}}{2})} \\ & \approx 2e^{i\mathbf{k}\cdot(\mathbf{z} - \frac{\mathbf{x}+\mathbf{y}}{2})} \left( 1 - e^{-i\mathbf{P}\cdot(\mathbf{x}-\mathbf{y})} \right), \quad (36) \end{aligned}$$

from which we immediately see that the scale of the coupling  $\mathbf{P}$  is given by the parent dipole size  $\mathbf{x} - \mathbf{y}$ . The physical interpretation of this is that the emission of the additional gluon happens coherently from the dipole (as evidenced by the fact that the kernel vanishes at  $\mathbf{x} = \mathbf{y}$ , reflecting color neutrality), thus the parent dipole determines the scale of the coupling. After changing the scale of the running coupling to  $\mathbf{x} - \mathbf{y}$  we can then pull it outside of the  $\mathbf{P}, \mathbf{k}$ -integral (32) and restore the exponential functions to the original form on the l.h.s. of Eq. (36). Doing this we get the estimate

$$\sim \alpha_s(\mathbf{x} - \mathbf{y}) \frac{(\mathbf{x} - \mathbf{y})^2}{(\mathbf{x} - \mathbf{z})^2 (\mathbf{y} - \mathbf{z})^2}, \quad |\mathbf{x} - \mathbf{y}| \ll |\mathbf{x} - \mathbf{z}| \approx |\mathbf{y} - \mathbf{z}| \quad (37)$$



for the kernel.

It is instructive to compare the estimate (34), (35) and (37) to the “Balitsky” rcBK equation, which reads, in our notation:

$$\begin{aligned} \partial_y \hat{D}_{\mathbf{x},\mathbf{y}}(y) = & \frac{N_c}{2\pi^2} \int_{\mathbf{z}} \left( \frac{\alpha_s(\mathbf{x}-\mathbf{z})\alpha_s(\mathbf{x}-\mathbf{y})}{\alpha_s(\mathbf{y}-\mathbf{z})} \mathbf{K}_{\mathbf{x}-\mathbf{z}}^2 \right. \\ & + \frac{\alpha_s(\mathbf{y}-\mathbf{z})\alpha_s(\mathbf{x}-\mathbf{y})}{\alpha_s(\mathbf{z}-\mathbf{y})} \mathbf{K}_{\mathbf{y}-\mathbf{z}}^2 \\ & \left. - 2\alpha_s(\mathbf{x}-\mathbf{y}) \mathbf{K}_{\mathbf{x}-\mathbf{z}} \cdot \mathbf{K}_{\mathbf{y}-\mathbf{z}} \right) \\ & \times \left[ \hat{D}(\mathbf{x},\mathbf{z})\hat{D}(\mathbf{z},\mathbf{y}) - \hat{D}(\mathbf{x},\mathbf{y}) \right]. \quad (38) \end{aligned}$$

One immediately recognizes that the scale of the coupling in the different kinematical limits is the same.

As a summary, showing the approximate equivalence of our rcJIMWLK equation, defined by Eqs. (25) and (26), to the “Balitsky” rcBK equation (38) commonly used in phenomenology involved the following steps. We first derived an equation for the two point function Eq. (27) that involved 4 transverse coordinates and a six-point function  $\hat{D}\hat{Q}$ . We subsequently took the limit of only 3 coordinates, instead of 4, for the Wilson line operators, reducing them to the BK form. We then identified the dominant momentum scales for the coupling in the kernel of Eq. (27) in the limits of small and large daughter dipoles compared to the parent dipole, and interchanged the momentum and the corresponding coordinate distance as the argument of the running coupling. In addition, our Eqs. (27) and (38) have been written as operator equations corresponding to the first equation of the infinite Balitsky hierarchy. While the JIMWLK equation solves the whole hierarchy simultaneously, a solution of just the BK equation requires one to truncate the hierarchy by replacing the operators  $\hat{D}$  by their expectation values. To quantify the effect of these approximations we shall now proceed to a comparison between numerical evaluations of the BK and JIMWLK equations.

## VII. NUMERICAL COMPARISON

The numerical algorithm for solving the JIMWLK equation is discussed in detail in [34], and the modifications required to adapt it to our version of the JIMWLK equation, Eqs. (25) and (26), are straightforward. We construct the initial condition Wilson line configurations as described in Ref. [38], using a  $1024^2$  transverse lattice, with the MV model parameter  $g^2\mu L = 31$  and the longitudinal extent in the MV model discretized in  $N_y = 100$  steps, leading to an initial fundamental representation saturation scale  $Q_s L \approx 22$ , where  $L$  is the size of the lattice in physical units. The infrared behavior of the

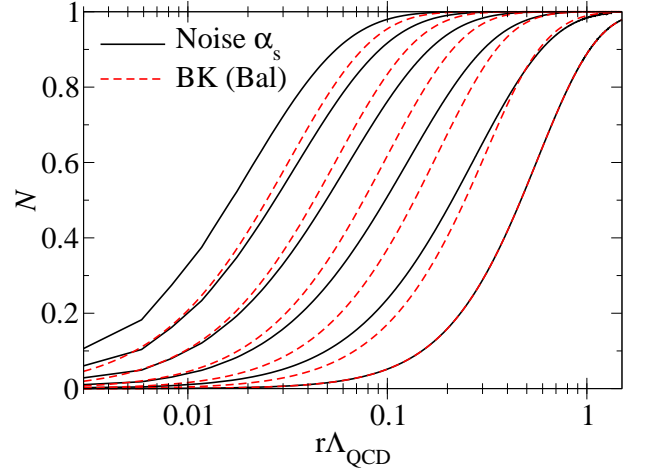


FIG. 5: Evolution of the scattering amplitude with the JIMWLK equation where the scale of the running coupling is set in the noise term, Eq. (24), compared to BK evolution with the “Balitsky” running coupling prescription, Eq. (38). The evolution is started from the same initial condition and the lines show the amplitude at intervals of 2 units in rapidity.

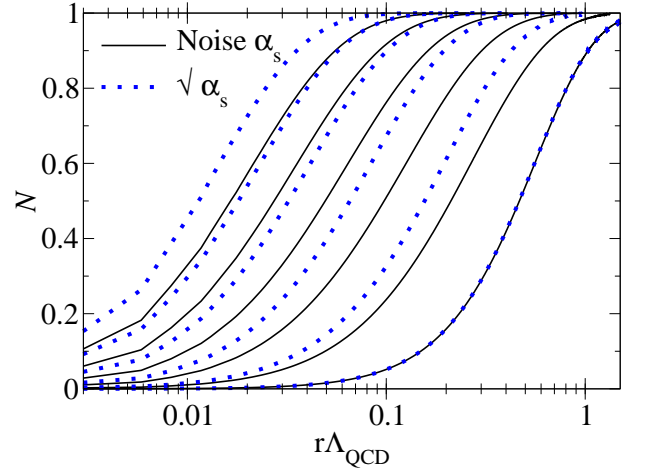


FIG. 6: Evolution of the scattering amplitude  $N \equiv 1 - \langle \hat{D}_{\mathbf{r}} \rangle$  with the rcJIMWLK equation proposed in this paper (same data as in Fig. 5), compared to the “square root” prescription (15) used in [11, 29]. The evolution is started from the same initial condition and the lines show the amplitude at intervals of 4 units in rapidity.

coupling is regularized as

$$\alpha_s(\mathbf{k}) = \frac{4\pi}{\beta \ln \left\{ \left[ \left( \frac{\mu_0^2}{\Lambda_{\text{QCD}}^2} \right)^{\frac{1}{c}} + \left( \frac{\mathbf{k}^2}{\Lambda_{\text{QCD}}^2} \right)^{\frac{1}{c}} \right]^c \right\}}, \quad (39)$$

with  $\beta = 11 - 2N_F/3$ , where we take  $N_F = 3$ . The parameter  $c = 0.2$  regulates the sharpness of the freezing of the coupling, which happens at  $\mu_0 L = 15$ . The value of the QCD scale is taken as  $\Lambda_{\text{QCD}} L = 6$ , leading to a value  $\alpha_0 = 0.7619$  for the coupling in the infrared. In the

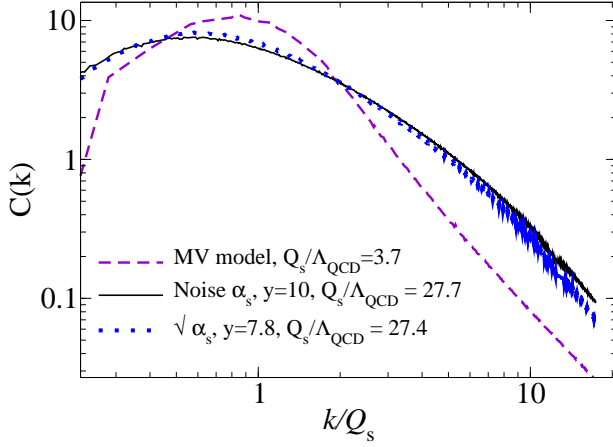


FIG. 7: The momentum space correlator, (41), from the rcJIMWLK equation proposed in this paper compared to the “square root” prescription (with the same parameters as used in Fig. 6). The correlator is shown for the initial condition, for which we use the MV model, and for  $y = 10$  and  $y = 7.8$  units of evolution for the two running coupling versions; these correspond to approximately the same value of  $Q_s$ . Note that the end of the curves at large  $k_T$  corresponds to the lattice ultraviolet cutoffs, and the shape is sensitive to lattice effects well below that.

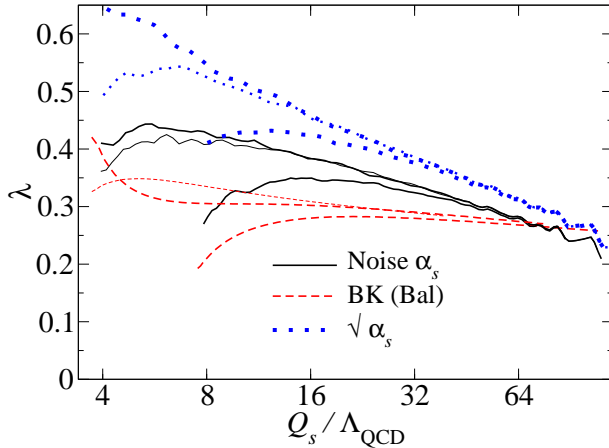


FIG. 8: Evolution speed of the saturation scale as a function of  $Q_s/\Lambda_{\text{QCD}}$ . Shown are the noise term (solid line), square root (dotted line) running coupling JIMWLK equations and the Balitsky prescription BK equation (dashed line), starting from the MV model at two different initial values of  $Q_s$ . The thin lines have the freezing of the coupling implemented more smoothly, with the value  $c = 1.5$  instead of  $c = 0.2$  as used elsewhere in this paper.

more extensive study in Ref. [29] the evolution speed was found to be very insensitive to the lattice parameters and to  $\alpha_0$  while naturally dependent on the physical ratio of scales  $Q_s/\Lambda_{\text{QCD}}$ .

When the coupling is needed as a function of the transverse coordinate, as in the BK equation or the  $\sqrt{\alpha_s}$ -prescription for JIMWLK that we study as a comparison,

we use

$$\alpha_s(\mathbf{r}) = \frac{4\pi}{\beta \ln \left\{ \left[ \left( \frac{\mu_0^2}{\Lambda_{\text{QCD}}^2} \right)^{\frac{1}{c}} + \left( \frac{4e^{-2\gamma_E}}{r^2 \Lambda_{\text{QCD}}^2} \right)^{\frac{1}{c}} \right]^c \right\}} \quad (40)$$

Note the constant factor  $4e^{-2\gamma_E} \approx 1.26$  in the identification  $k_T^2 \sim 4e^{-2\gamma_E}/r_T^2$ , which is taken from the explicit Fourier-transform of the kernel in Refs. [19, 39]. In Appendix A we show a comparison between the coordinate and momentum versions of the running coupling, verifying that this is indeed the correct correspondence. Phenomenological studies typically [22, 23] find that the coordinate space scale needs to be taken as larger,  $\sim 20/r_T^2$  for  $\Lambda_{\text{QCD}} \gtrsim 200\text{MeV}$ , unless some other corrections are applied that slow down the evolution, such as in Ref. [25]. Thus, in spite of the slowness of the rcBK evolution with the Balitsky prescription compared to fixed coupling, the data seems to prefer a slower evolution still than it would predict.

Figure 5 compares the evolution of the dipole using the rcJIMWLK equation (Eqs. (25) and (26) with (39) for the coupling) with the Balitsky prescription rcBK equation (38) with the coupling (40) over 20 units in rapidity. We see that the Balitsky prescription leads still to a slower evolution than our proposal, in spite of the similarity in parametrically different parts of the phase space discussed above. Discretization effects that also affect the comparison are discussed in Appendix A. The shape of the correlator as a function of  $r_T$  is steeper in BK than in JIMWLK, for which we do not see a compelling explanation.

Figure 6 compares the rcJIMWLK evolution using our proposal to the “square root” coupling (15) used in previous rcJIMWLK calculations [11, 29]. One can see that the evolution speed is slowed down significantly from the “square root” prescription. While the shape of the front seems somewhat different there is no clear sign of a different power law in the momentum space correlator

$$C(\mathbf{k}) = \mathbf{k}^2 \int d^2\mathbf{r} e^{i\mathbf{k}\cdot\mathbf{r}} \langle \hat{D}(r_T) \rangle. \quad (41)$$

This is shown in Fig. 7 as a function of the scaling variable  $k_T/Q_s$  for both coupling constant prescriptions at a similar value of  $Q_s$  (which, due to the different evolution speed, correspond to slightly different values of rapidity). More detailed statements on the geometric scaling behavior at large  $k_T$  would require significantly larger lattices to push out the  $\sim 1/a$  ultraviolet cutoff further.

Figure 8 further illustrates the difference in evolution speeds between the prescriptions. The evolution speed is defined as

$$\lambda \equiv \frac{d \ln Q_s^2}{dy}, \quad (42)$$

with the saturation scale  $Q_s$  solved from the condition

$$\langle \hat{D}(r_T^2 = 2/Q_s^2) \rangle = e^{-1/2}. \quad (43)$$

In addition to the initial condition used in Fig. 6, evolved for 20 units in  $y$ , Fig. 8 also shows the result of a calculation started with an initial  $Q_s$  twice as large. The evolution speed shows the typical behavior also seen with the BK equation (see e.g. [25, 40]), with a slower evolution in the initial transient region when the dipole cross section changes from the initial condition to the pseudoscaling form, followed by a universal  $1/\sqrt{y}$ -dependence characteristic of rcBK evolution. For comparison Fig. 8 also shows the evolution speed calculated with a smoother freezing of the coupling in the infrared, implemented by choosing  $c = 1.5$  in Eqs. (39) and (40). The dependence on the freezing prescription, which is not present for larger initial  $Q_s/\Lambda_{\text{QCD}}$  (not shown on the figure) is, interestingly, different for the BK and JIMWLK calculations. This initial behavior of course also depends on the functional form of the initial condition. At large rapidities, the evolution speed in JIMWLK drops below that in BK due to the fact that  $Q_s$  grows close to the lattice ultraviolet cutoff; see the discussion in Appendix A.

We remind the reader that the typical phenomenologically favored initial saturation scale for the evolution is  $Q_s \sim 1$  GeV and the evolution speed resulting from fits to HERA data (e.g. [22, 23, 25, 41–43]) is  $\lambda \sim 0.2 \dots 0.3$ . The “square root” coupling could be made to fit experimental data by adjusting the coefficient under the logarithm in the running coupling as  $\ln[4C^2/(r^2\Lambda_{\text{QCD}}^2)]$  effectively taking  $\Lambda_{\text{QCD}}$  as a fit parameter. Doing so would, however, lead to an unnaturally large value for  $C$ , i.e. small value for the effective  $\Lambda_{\text{QCD}}$ . With our rcJIMWLK prescription, as with the Balitsky rcBK, this problem is much less severe, although still present to some degree.

### VIII. CONCLUSIONS

Until now running coupling solutions of the JIMWLK equation have been limited by the belief that since the Langevin formulation is written in terms of the square root of the JIMWLK kernel, one is limited to considering only prescriptions that modify this square root. In particular, since the square root only depends on the size of the daughter dipole, it has been impossible to include a dependence on the “parent” dipole size in the coupling. We have in this paper pointed out that there is in fact another scale also in the Langevin formulation that the running coupling can depend on, namely the scale in the random noise term. We have proposed to use this scale as the argument of the running coupling, with the Langevin timestep of the JIMWLK equation given by Eqs. (25) and (26). Choosing this as the scale of the coupling has several advantages. Firstly it corresponds naturally to the general argument that the scale of the coupling should be the momentum of the emitted gluon. Secondly we have shown analytically how it leads to the typical scale of the coupling being taken as the smallest one of the three relevant dipole sizes (the “parent” and two “daughter” dipoles) present in a dipole splitting. This is very similar

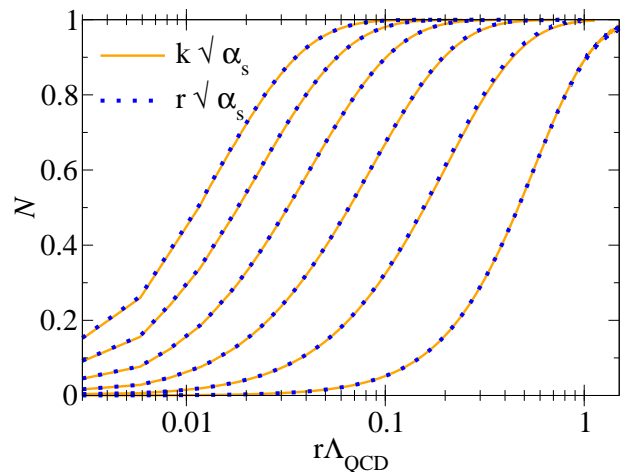


FIG. 9: Evolution of the scattering amplitude  $N \equiv 1 - \langle \hat{D}_r \rangle$  with the “square root” coupling rcJIMWLK equation, with coupling evaluated at the scale  $k_T^2$  in the momentum space kernel, and at the scale  $4e^{-2\gamma_E}/r_T^2$  in the position space kernel.

to the “Balitsky” prescription for the running coupling in the BK equation. We have shown numerically that the evolution speed of the saturation scale in our proposed running coupling JIMWLK equation is slower than the “square root” coupling, although not fully consistent with the Balitsky prescription for BK, or with fits of the data [22, 23].

### Acknowledgements

T.L. thanks F. Gelis for discussions and IPhT, CEA/Saclay (URA du CNRS) for hospitality during the early stage of this work. H.M. is supported by the Graduate School of Particle and Nuclear Physics. This work has been supported by the Academy of Finland, project 133005, and by computing resources from CSC – IT Center for Science in Espoo, Finland.

### Appendix A: Lattice effects

As test of the equivalence of the scales  $k_T^2$  in the momentum space coupling and the scale  $4e^{-2\gamma_E}/r_T^2$  in coordinate space we show in Fig. 9 a comparison between a solution of the rcJIMWLK equation using the two couplings. This can be done straightforwardly when one uses the “square root” coupling, where one can easily multiply either the kernel  $\mathbf{K}_x$  or its Fourier-transform with  $\sqrt{\alpha_s}$ . Thus the curves in Fig. 9 correspond to evolution using the kernels

$$\sqrt{\alpha_s(\mathbf{r})}\mathbf{K}_r, \quad (\text{A1})$$

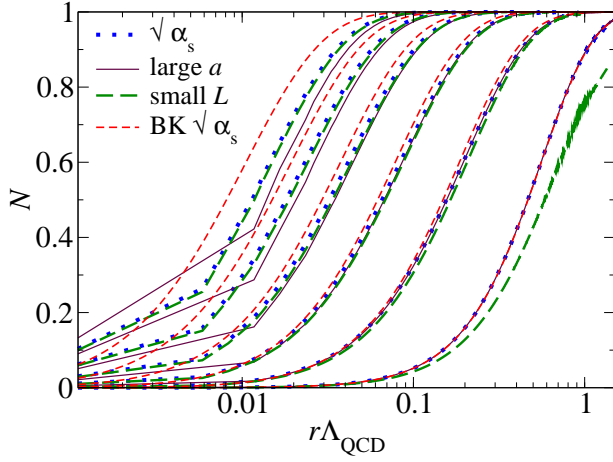


FIG. 10: Evolution of the scattering amplitude  $N \equiv 1 - \langle \hat{D}_r \rangle$  with the “square root” rcJIMWLK equation (dotted line) and with the BK equation (thinner dashed line) using the same “square root” running coupling. The initial condition is the same as in Fig. 6 and the amplitude is shown every 4 units in  $y$ . Also shown are JIMWLK simulations on a smaller  $512^2$ -lattice with the physical lattice size reduced (“small  $L$ ”, thick dashed line) or lattice spacing increased (“large  $a$ ”, thin solid line) by a factor 2.

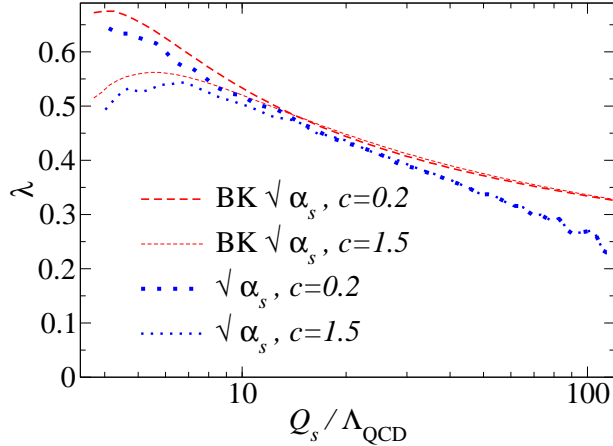


FIG. 11: Evolution speed of the saturation scale  $\lambda$  with the “square root” coupling. Shown are the results from the BK and JIMWLK simulations with the same kernel, using infrared regularizations of the running coupling with different values of the parameter  $c$ .

labeled  $r\sqrt{\alpha_s}$ , and

$$i(2\pi)^2 \int \frac{d^2\mathbf{k}}{(2\pi)^2} \sqrt{\alpha_s(\mathbf{k})} \frac{e^{-i\mathbf{k}\cdot\mathbf{x}}}{\mathbf{k}^2}, \quad (\text{A2})$$

labeled  $k\sqrt{\alpha_s}$ , with  $\alpha_s(\mathbf{x})$  and  $\alpha_s(\mathbf{k})$  given by Eqs. (39) and (40). They are seen to agree remarkably well, just

tifying our use of the constant  $4e^{-2\gamma_E}$  in comparing the momentum and position space formulations.

The BK equation is solved on a logarithmic grid in  $r_T$ , with the values of the scattering amplitude between the grid points obtained from interpolation. This allows one in practice to study as small or large  $r_T$ -values as desired. In the case of JIMWLK, on the other hand, one works on a fixed linear lattice with cutoffs  $\sim 1/L$  in the infrared and  $\sim 1/a$  in the ultraviolet. One expects large lattice effects when  $Q_s \sim 1/L$  and when  $Q_s \sim 1/a$ , and since  $Q_s$  changes exponentially during the evolution, this restricts the accessible rapidity range.

To illustrate the numerical uncertainties in our calculation we compare in Fig. 10 the rcJIMWLK calculation with a square root running coupling, shown also in Fig. 6, to the BK equation with the same running coupling prescription. One can see that the solutions agree very well for smaller rapidities, but start to deviate more later in the evolution. Also shown is a rcJIMWLK calculation with the same initial  $g^2\mu/\Lambda_{\text{QCD}}$  (approximately the same  $Q_s/\Lambda_{\text{QCD}}$ ) performed on a smaller  $512^2$ -lattice in such a way that either the IR  $\sim 1/L$  or UV  $\sim 1/a$  cutoff is different. We see that for the initial condition  $Q_s$  is so small that changing the IR cutoff starts to have an effect. More importantly, late in the evolution the solution becomes sensitive to the UV cutoff; an extrapolation to  $a \rightarrow 0$  would bring the JIMWLK result closer to BK.

A further comparison of the evolution speed in the BK and rcJIMWLK codes is shown in Fig. 11. It can be seen that in BK the evolution is slightly faster, and increasingly so at large  $Q_s$ , when the lattice ultraviolet cutoff in the JIMWLK code slows down the evolution. In a JIMWLK simulation closer to the continuum limit the difference would be smaller. The figure also demonstrates the dependence on the parameter  $c$  controlling the smoothness of the infrared regularization of the coupling. As was seen previously in Fig. 8, the evolution speed is sensitive to the regularization for small  $Q_s/\Lambda_{\text{QCD}}$ .

In addition, the BK and JIMWLK equations are not equivalent even in the continuum, because of the mean field approximation. Making a precise statement about this difference would require a more systematical extrapolation of the lattice calculation to the continuum and infinite volume limits than is done here. For fixed coupling the difference in the evolution speed between the BK and JIMWLK equations has been studied in Ref. [35], where JIMWLK evolution was found to be slower by few per cent, while an even smaller difference was seen for running coupling in Ref. [44].



- [2] T. Lappi *Int. J. Mod. Phys. E* **20** (2011) 1 [[arXiv:1003.1852 \[hep-ph\]](#)].
- [3] J. Jalilian-Marian, A. Kovner, L. D. McLerran and H. Weigert *Phys. Rev. D* **55** (1997) 5414 [[arXiv:hep-ph/9606337](#)]; J. Jalilian-Marian, A. Kovner, A. Leonidov and H. Weigert *Nucl. Phys. B* **504** (1997) 415 [[arXiv:hep-ph/9701284](#)]; J. Jalilian-Marian, A. Kovner, A. Leonidov and H. Weigert *Phys. Rev. D* **59** (1999) 014014 [[arXiv:hep-ph/9706377](#)]; J. Jalilian-Marian, A. Kovner and H. Weigert *Phys. Rev. D* **59** (1999) 014015 [[arXiv:hep-ph/9709432](#)]; J. Jalilian-Marian, A. Kovner, A. Leonidov and H. Weigert *Phys. Rev. D* **59** (1999) 034007 [[arXiv:hep-ph/9807462](#)]; E. Iancu, A. Leonidov and L. D. McLerran *Nucl. Phys. A* **692** (2001) 583 [[arXiv:hep-ph/0011241](#)]; E. Iancu and L. D. McLerran *Phys. Lett. B* **510** (2001) 145 [[arXiv:hep-ph/0103032](#)]; E. Ferreira, E. Iancu, A. Leonidov and L. McLerran *Nucl. Phys. A* **703** (2002) 489 [[arXiv:hep-ph/0109115](#)]; E. Iancu, A. Leonidov and L. D. McLerran *Phys. Lett. B* **510** (2001) 133 [[arXiv:hep-ph/0102009](#)].
- [4] H. Weigert *Nucl. Phys. A* **703** (2002) 823 [[arXiv:hep-ph/0004044 \[hep-ph\]](#)].
- [5] A. H. Mueller *Phys. Lett. B* **523** (2001) 243 [[arXiv:hep-ph/0110169](#)].
- [6] I. Balitsky *Nucl. Phys. B* **463** (1996) 99 [[arXiv:hep-ph/9509348](#)].
- [7] Y. V. Kovchegov *Phys. Rev. D* **60** (1999) 034008 [[arXiv:hep-ph/9901281](#)].
- [8] Y. V. Kovchegov *Phys. Rev. D* **61** (2000) 074018 [[arXiv:hep-ph/9905214](#)].
- [9] C. Marquet *Nucl. Phys. A* **796** (2007) 41 [[arXiv:0708.0231 \[hep-ph\]](#)].
- [10] J. L. Albacete and C. Marquet *Phys. Rev. Lett.* **105** (2010) 162301 [[arXiv:1005.4065 \[hep-ph\]](#)].
- [11] A. Dumitru, J. Jalilian-Marian, T. Lappi, B. Schenke and R. Venugopalan *Phys. Lett. B* **706** (2011) 219 [[arXiv:1108.4764 \[hep-ph\]](#)].
- [12] F. Dominguez, C. Marquet, B.-W. Xiao and F. Yuan *Phys. Rev. D* **83** (2011) 105005 [[arXiv:1101.0715 \[hep-ph\]](#)].
- [13] T. Lappi and H. Mäntysaari [arXiv:1209.2853 \[hep-ph\]](#).
- [14] A. Dumitru, F. Gelis, L. McLerran and R. Venugopalan *Nucl. Phys. A* **810** (2008) 91 [[arXiv:0804.3858 \[hep-ph\]](#)].
- [15] F. Gelis, T. Lappi and R. Venugopalan *Phys. Rev. D* **79** (2008) 094017 [[arXiv:0810.4829 \[hep-ph\]](#)].
- [16] K. Dusling, F. Gelis, T. Lappi and R. Venugopalan *Nucl. Phys. A* **836** (2010) 159 [[arXiv:0911.2720 \[hep-ph\]](#)].
- [17] A. Dumitru, K. Dusling, F. Gelis, J. Jalilian-Marian, T. Lappi and R. Venugopalan *Phys. Lett. B* **697** (2011) 21 [[arXiv:1009.5295 \[hep-ph\]](#)].
- [18] K. Dusling and R. Venugopalan *Phys. Rev. Lett.* **108** (2012) 262001 [[arXiv:1201.2658 \[hep-ph\]](#)].
- [19] Y. V. Kovchegov and H. Weigert *Nucl. Phys. A* **784** (2007) 188 [[arXiv:hep-ph/0609090](#)].
- [20] I. Balitsky *Phys. Rev. D* **75** (2007) 014001 [[arXiv:hep-ph/0609105](#)].
- [21] J. L. Albacete and Y. V. Kovchegov *Phys. Rev. D* **75** (2007) 125021 [[arXiv:0704.0612 \[hep-ph\]](#)].
- [22] J. L. Albacete, N. Armesto, J. G. Milhano and C. A. Salgado *Phys. Rev. D* **80** (2009) 034031 [[arXiv:0902.1112 \[hep-ph\]](#)].
- [23] J. L. Albacete, N. Armesto, J. G. Milhano, P. Quiroga-Arias and C. A. Salgado *Eur. Phys. J. C* **71** (2011) 1705 [[arXiv:1012.4408 \[hep-ph\]](#)].
- [24] J. L. Albacete and C. Marquet *Phys. Lett. B* **687** (2010) 174 [[arXiv:1001.1378 \[hep-ph\]](#)].
- [25] J. Kuokkanen, K. Rummukainen and H. Weigert *Nucl. Phys. A* **875** (2012) 29 [[arXiv:1108.1867 \[hep-ph\]](#)].
- [26] J. L. Albacete, A. Dumitru, H. Fujii and Y. Nara [arXiv:1209.2001 \[hep-ph\]](#).
- [27] I. Balitsky and G. A. Chirilli *Phys. Rev. D* **77** (2008) 014019 [[arXiv:0710.4330 \[hep-ph\]](#)].
- [28] E. Avsar, A. Stasto, D. Triantafyllopoulos and D. Zaslavsky *JHEP* **1110** (2011) 138 [[arXiv:1107.1252 \[hep-ph\]](#)].
- [29] T. Lappi *Phys. Lett. B* **703** (2011) 325 [[arXiv:1105.5511 \[hep-ph\]](#)].
- [30] A. Kovner and M. Lublinsky *JHEP* **0503** (2005) 001 [[arXiv:hep-ph/0502071 \[hep-ph\]](#)].
- [31] A. Kovner and M. Lublinsky *Phys. Rev. Lett.* **94** (2005) 181603 [[arXiv:hep-ph/0502119 \[hep-ph\]](#)].
- [32] E. Iancu and D. Triantafyllopoulos *JHEP* **1204** (2012) 025 [[arXiv:1112.1104 \[hep-ph\]](#)].
- [33] J.-P. Blaizot, E. Iancu and H. Weigert *Nucl. Phys. A* **713** (2003) 441 [[arXiv:hep-ph/0206279 \[hep-ph\]](#)].
- [34] K. Rummukainen and H. Weigert *Nucl. Phys. A* **739** (2004) 183 [[arXiv:hep-ph/0309306 \[hep-ph\]](#)].
- [35] Y. V. Kovchegov, J. Kuokkanen, K. Rummukainen and H. Weigert *Nucl. Phys. A* **823** (2009) 47 [[arXiv:0812.3238 \[hep-ph\]](#)].
- [36] C. Marquet and H. Weigert *Nucl. Phys. A* **843** (2010) 68 [[arXiv:1003.0813 \[hep-ph\]](#)].
- [37] J. W. Cooley and J. W. Tukey *Math. Comput.* **19** (1965) 297.
- [38] T. Lappi *Eur. Phys. J. C* **55** (2008) 285 [[arXiv:0711.3039 \[hep-ph\]](#)].
- [39] E. Gardi, J. Kuokkanen, K. Rummukainen and H. Weigert *Nucl. Phys. A* **784** (2007) 282 [[arXiv:hep-ph/0609087 \[hep-ph\]](#)].
- [40] J. L. Albacete *Phys. Rev. Lett.* **99** (2007) 262301 [[arXiv:0707.2545 \[hep-ph\]](#)].
- [41] K. J. Golec-Biernat and M. Wusthoff *Phys. Rev. D* **59** (1999) 014017 [[arXiv:hep-ph/9807513](#)].
- [42] E. Iancu, K. Itakura and S. Munier *Phys. Lett. B* **590** (2004) 199 [[arXiv:hep-ph/0310338](#)].
- [43] G. Soyez *Phys. Lett. B* **655** (2007) 32 [[arXiv:0705.3672 \[hep-ph\]](#)].
- [44] J. Kuokkanen. PhD thesis, University of Oulu, 2011.